ACS SyntheticBiology

pubs.acs.org/synthbio Research Article

Glycosylation of Structured Protein Domains in Cell-Free Reaction Environments

Erik J. Bidstrup, Kyle Hill, Chandra K. Bandi, D. Natasha Owitipana, Alina Chisti, Rochelle Aw, Xu Yang, Parastoo Azadi, Michael C. Jewett, Lai-Xi Wang, Weston Kightlinger, and Matthew P. DeLisa*

Cite This: *ACS Synth. Biol.* 2025, 14, 2354–2367 Read Online

ACCESS | Metrics & More | Article Recommendations | Supporting Information

ABSTRACT: The production of *N*-linked glycoproteins in genetically tractable bacterial hosts and their cell-free extracts holds great promise for low-cost, customizable, and distributed biomanufacturing of glycoconjugate vaccines and glycoprotein therapeutics. In nearly all bacterial *N*-linked protein glycosylation systems described so far, a single-subunit, transmembrane oligosaccharyltransferase (OST) is employed which favors acceptor sites in flexible, solvent-exposed motifs of the glycoprotein substrate. Yet despite this preference, acceptor sites in structured domains can also be glycosylated in living bacteria, presumably by a mechanism where the site is presented to the OST in a flexible form during or after the membrane translocation step but prior to folding being completed. While *N*-glycoprotein biosynthesis can also be accomplished using cell-free extracts derived from glycosylation-competent bacteria, it remains to be determined whether the cell-free reaction environment involves a similar mechanism for glycosylation of structured domains. Using an *Escherichia coli*-based cell-free glycoprotein synthesis (CFGpS) system, we observed efficient glycosylation of two eukaryotic glycoproteins, namely ribonuclease A (RNase A) and the fragment crystallizable (Fc) region of human immunoglobulin G (IgG), whose acceptor sites occur in structurally constrained regions that were not glycosylated when the proteins were already folded. Because this cell-free glycosylation depended on ribosomal translation but not on signal peptide-mediated translocation, we propose the existence of a unique co-translational, but not co-translocational, glycosylation mechanism in CFGpS. Collectively, these findings reveal the potential for CFGpS to become a viable platform for producing complex eukaryotic glycoprotein targets.

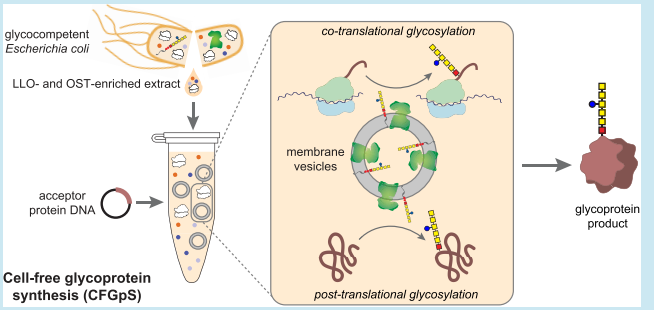

KEYWORDS: *asparagine-linked (N-linked) glycosylation, cell-free protein synthesis (CFPS), glycoprotein, immunoglobulin, protein folding, synthetic glycobiology*

INTRODUCTION

In recent years, multiple biomanufacturing paradigms have emerged that enable decentralized and potentially portable production of protein therapeutics and vaccines.[1−5] While these point-of-care technologies have been used to make a range of important therapeutic proteins such as erythropoietin, human growth hormone, and interferon alpha-2b, their inability to execute controllable and reproducible glycosylation has limited the spectrum of therapeutically relevant proteins that can be furnished by these systems. The significance of this shortcoming is underscored by the fact that most clinically approved protein therapeutics harbor glycans that are attached to either asparagine residues (*N*-linked glycans) or serine/threonine residues (*O*-linked glycans)[6] and are known to impact critical therapeutic properties including pharmacokinetics, immunogenicity, and biological activity.[7−10] Due to the important roles that glycosylation plays in therapeutic efficacy, methods for on-demand production of proteins with defined glycosylation are an unmet biotechnological need.

To address this need, we recently developed a technology called cell-free glycoprotein synthesis (CFGpS) that integrates protein biosynthesis with *N*-linked protein glycosylation in a single-pot reaction.[11] CFGpS leverages *Escherichia coli* strains that are rendered capable of glycosylation (glycocompetent *E. coli*) to source extracts that are selectively enriched with glycosylation components, including oligosaccharyltransferases (OSTs) and lipid-linked oligosaccharides (LLOs). When supplemented with plasmid DNA encoding a recombinant acceptor protein, the extract containing enriched glycosylation machinery is capable of transferring glycans onto newly synthesized target proteins. Importantly, the modularity of

Received: March 30, 2025
Revised: May 22, 2025
Accepted: May 23, 2025
Published: May 28, 2025

https://doi.org/10.1021/acssynbio.5c00229
ACS Synth. Biol. 2025, 14, 2354−2367

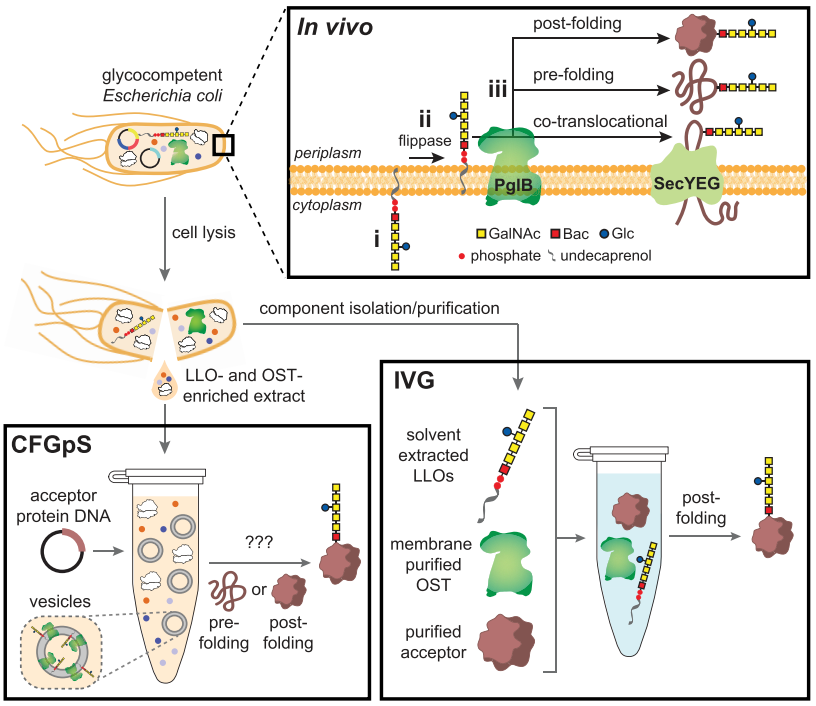

Figure 1. Glycosylation mechanisms in bacterial cell-based and cell-free expression systems. Schematic of cell-based glycosylation (*in vivo*) versus cell-free glycosylation using either component isolation/purification (IVG) or extracts that integrate transcription, translation, and glycosylation (CFGpS). *In vivo* glycosylation involves: (i) assembly of a lipid-linked oligosaccharide (LLO) on the cytoplasmic face of the inner membrane that is (ii) flipped into the periplasm where it serves as a donor for the OST (e.g., PglB), which (iii) transfers the glycan onto asparagine residues in acceptor proteins either during translocation (co-translocational), following translocation but before folding is complete (pre-folding), or following translocation after folding is completed (post-folding). IVG makes use of solvent extracted LLOs, membrane purified OSTs, and purified acceptor proteins to achieve *N*-linked glycosylation that occurs entirely post-folding. CFGpS integrates transcription, translation, and glycosylation of acceptor proteins in a cell-like environment using extracts enriched with membrane vesicles containing LLOs and OST.

CFGpS allows facile assembly and prototyping of natural and synthetic glycosylation pathways composed of distinct OSTs and structurally diverse LLOs for rapid biosynthesis of a wide range of glycoprotein products,[12−15] including conjugate vaccines.[16−18] However, while the glycosylation competence of CFGpS systems has been established, the mechanism of *N*-glycan attachment in the cell-free environment and how it compares to the cellular context remains poorly understood.

Previous studies have revealed that glycosylation efficiency of substrate proteins by the canonical bacterial OST from *Campylobacter jejuni*, PglB (*Cj*PglB), is highly dependent on the structural context of the target sequon. For example, the model *C. jejuni* glycoprotein, AcrA, which harbors two acceptor sequons that are in flexible, solvent-exposed motifs, was efficiently glycosylated in living *E. coli* cells carrying *Campylobacter jejuni*-derived glycosylation machinery (hereafter *in vivo*).[19] Interestingly, *in vivo* glycosylation of AcrA was observed: (1) long after signal peptide removal, suggesting some level of post-translocational glycosylation; and (2) following export of fully folded AcrA via the twin-arginine translocation (Tat) system, suggesting *Cj*PglB can glycosylate an already folded protein. In line with this latter finding, independently expressed and purified AcrA was efficiently glycosylated following incubation with purified *Cj*PglB and a crude lipid extract containing LLOs modified with the *C. jejuni* heptasaccharide glycan (hereafter *in vitro* glycosylation or IVG),[19] confirming the accessibility of the sequon in folded AcrA. For other model acceptor proteins like *C. jejuni* PEB3 and bovine ribonuclease A (RNase A), which harbor glycan acceptor sites in highly structured domains of the protein, efficient glycosylation was also observed *in vivo* but hardly any glycosylation (∼1%) was detected in IVG.[19−21] Thus, unlike the sequons in AcrA, those in PEB3 and RNase A were inaccessible to *Cj*PglB after the proteins were folded. Consequently, the *Cj*PglB-mediated installation of glycans on PEB3 and RNase A, as was observed *in vivo*, must occur before acceptor protein folding has completed (e.g., during or shortly after membrane translocation) or following partial destabilization of the folded protein[20−23] (Figure 1). Indeed, one possible mechanism whereby translation, translocation and glycosylation are closely coordinated, as is common in eukaryotes,[24] was previously proposed to explain *in vivo* glycosylation of sequons in highly structured or solvent-inaccessible regions by the bacterial OST.[20]

Whether the CFGpS environment can similarly support glycosylation of sequons in highly structured or solvent-inaccessible regions remains unknown. However, because sequons frequently occur in structured or solvent-inaccessible regions of glycoproteins,[25] the existence of such a mechanism would have important consequences for the utility of CFGpS. Accordingly, in this work we investigated the ability of CFGpS to promote *N*-linked glycosylation of sequons positioned near structural features that make them challenging targets for the bacterial OST. To this end, we focused on bovine RNase A and a hinge-Fc fragment derived from human IgG, both of which were mutated to create an optimal bacterial acceptor sequence at their native *N*-glycosylation sites. As expected, neither RNase A nor hinge-Fc was glycosylated when provided to an IVG reaction in a completely folded conformation. On the other hand, strong glycosylation was observed when each

https://doi.org/10.1021/acssynbio.5c00229
ACS Synth. Biol. 2025, 14, 2354−2367

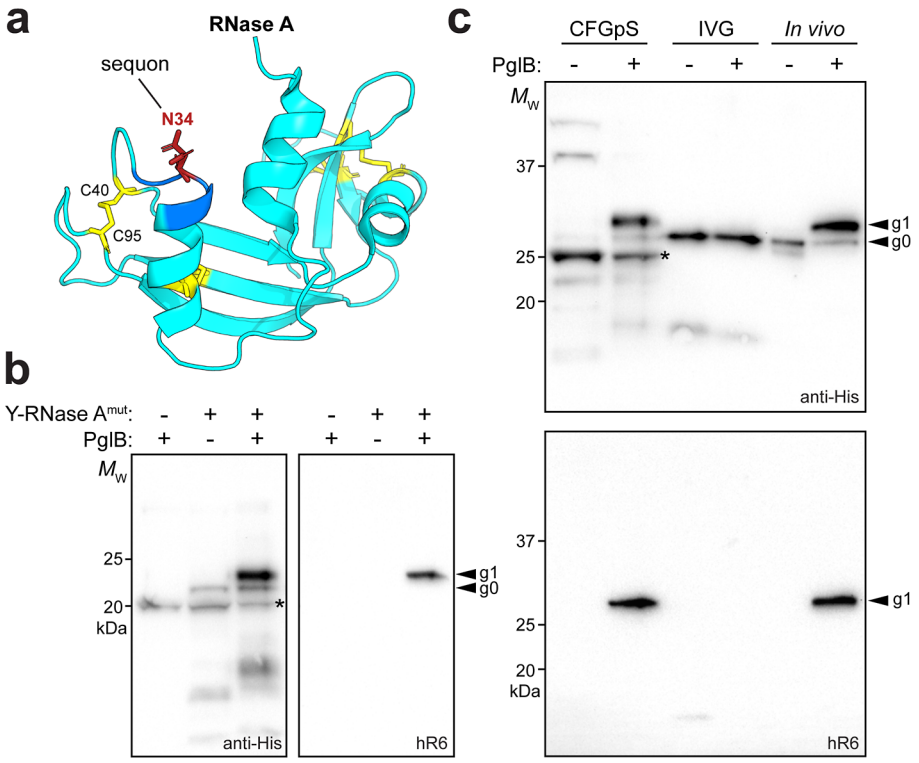

Figure 2. Efficient glycosylation of structured domain in RNase A using CFGpS. (a) Crystal structure of wild-type (wt) RNase A (PDB ID: 1KF5) in cyan, with disulfide bonds highlighted in yellow, sequon in blue, and glycosylated asparagine residue in red. Reproduced from Pratama et al.[23] Available under a Creative Commons Attribution 4.0 International License CC-BY license, copyright 2021, F. Pratama, D. Linton and N. Dixon. (b) Immunoblot analysis of YebF-RNase $A^{H12A/S32D}$ (Y-RNase A^{mut}) produced in CFGpS S12 lysates enriched with *Cj*LLOs, with (+) or without (−) *Cj*PglB, and with (+) or without (−) the acceptor protein expression plasmid, pJL1-YebF-RNase $A^{H12A/S32D}$. (c) Immunoblot analysis of YebF-RNase $A^{H12A/S32D}$ glycosylation in CFGpS, IVG, and *in vivo* systems. CFGpS was performed as in (b). IVG was performed using aglycosylated YebF-RNase $A^{H12A/S32D}$ purified from BL21(DE3), solvent extracted *Cj*LLOs, and membrane purified *Cj*PglB. *In vivo* glycosylation was performed using CLM24 cells carrying plasmid pTrc99S-YebF-RNase $A^{H12A/S32D}$ for YebF-RNase $A^{H12A/S32D}$ expression, pMW07-pglΔB for producing *Cj*LLOs, and either pMAF10 for wt *Cj*PglB expression (+) or an analogous plasmid that expresses $CjPglB^{mut}$ (−), a catalytically inactive mutant of *Cj*PglB described in Ollis et al.[27] All blots were probed with either polyhistidine epitope tag-specific antibody (anti-His) to detect the C-terminal 6x-His tag on YebF-RNase $A^{H12A/S32D}$ or anti-glycan serum (hR6) to detect the *C. jejuni* heptasaccharide glycan. Molecular weight (M_W) markers are indicated on the left. The g0 (27.7 kDa) and g1 (29.1 kDa) arrows indicate aglycosylated and monoglycosylated acceptor proteins, respectively, while the asterisk denotes a background band in the anti-His blots unrelated to YebF-RNase $A^{H12A/S32D}$. Blots are representative of biological replicates (n = 3).

protein was expressed in CFGpS, with glycosylation efficiencies on par with that observed following expression in glyco-competent *E. coli*. Based on these and other data, we propose a model in which glycosylation in CFGpS happens either while the nascent polypeptide is emerging from the ribosome (co-translational) or shortly after the nascent chain exits the ribosome but before it has reached its final folded confirmation (pre-folding). Overall, these results not only shed important light on mechanistic aspects of *N*-linked glycosylation in the CFGpS environment but also opens future possibilities for the biosynthesis of complex biopharmaceutical products such as IgG antibodies with customized glycosylation.

RESULTS

CFGpS Supports Glycosylation of Bovine RNase A. To better understand the glycosylation mechanism in CFGpS (Figure 1), we first focused our attention on bovine RNase A as a model acceptor protein because: (i) it is a native glycoprotein with a single ^{32}SRNLT^{36} sequon that occurs within a structured region of the protein created in part by adjacent disulfide bonds (Figure 2a);[26] (ii) RNase A variants engineered with bacterial consensus sequons, either an S32D substitution or a recoded ^{32}DQNAT ^{36} motif, can be glycosylated *in vivo* by *Cj*PglB;[21,22,27] and (iii) folded conformations of these RNase A variants are recalcitrant to IVG with isolated/purified components,[19,21] indicating that the N34 glycosylation site is inaccessible to *Cj*PglB in already folded RNase A. To further adapt RNase A^{S32D}[19,22] for CFGpS, we introduced an H12A substitution to inactivate the endoribonuclease activity of RNase A,[28] which was required to prevent destruction of important RNA substrates in the cell-free reaction (Figure S1). Lastly, a YebF secretion domain[29] was introduced at the N-terminus of RNase A to allow direct comparison with the construct used for *in vivo* glycosylation, which requires translocation to the periplasm. Moreover, we speculated that the YebF domain could be important for targeting the protein to the translocation machinery in cell-derived membrane vesicles (∼100 nM in diameter) that are present in CFGpS extracts.[12] Increasing the concentration of these vesicles is known to promote increased glycosylation efficiency and glycoprotein yields, presumably due to their highly enriched concentrations of enzymes involved in glycosylation and translocation.

Expression of the resulting YebF-RNase $A^{H12A/S32D}$ construct required a suitable cell-free extract that could co-activate

https://doi.org/10.1021/acssynbio.5c00229
ACS Synth. Biol. 2025, 14, 2354−2367

protein synthesis, glycosylation, and disulfide bond formation, with the latter needed for the introduction of the four native disulfide bonds that are essential for the conformational stability and catalytic activity of RNase A.[30] To this end, we chose to source cell-free extracts from *E. coli* SHuffle T7 Express, a *trxB gor* suppressor stain that has diminished cytoplasmic reductive activity and constitutively expresses disulfide bond isomerase C (DsbC) in the cytoplasm.[31] As a result, SHuffle T7 Express enables cytoplasmic expression of complex disulfide bonded proteins[31,32] and, moreover, extracts from this strain can better support disulfide bond formation in cell-free reactions.[33] Here, CFGpS lysate was produced from SHuffle T7 Express cells expressing *Cj*PglB and the biosynthetic pathway for the *C. jejuni* heptasaccharide glycan composed of $GalNAc_5$(Glc)diNAcBac (Figure 1). This lysate, which contained lipid-linked *C. jejuni* glycan (hereafter *Cj*LLOs) and active *Cj*PglB, was used to catalyze CFGpS reactions primed with a plasmid encoding pJL1-YebF-RNase $A^{H12A/S32D}$. Glycosylation of the YebF-RNase $A^{H12A/S32D}$ fusion protein was evaluated by immunoblot analysis with a polyhistidine epitope tag-specific antibody (anti-His) and *C. jejuni* heptasaccharide-specific serum (hR6).[34] Using the anti-His antibody, we detected the aglycosylated (g0) and monoglycosylated (g1) forms of YebF-RNase $A^{H12A/S32D}$ in the reaction mixture, while the higher molecular weight g1 band was detected with hR6 serum (Figure 2b). Control reactions were performed with lysates from cells that lacked either the plasmid encoding the target protein YebF-RNase $A^{H12A/S32D}$ or the *Cj*PglB enzyme. In both cases, no detectable glycosylation was observed (Figure 2b). These results establish that YebF-RNase $A^{H12A/S32D}$ can be efficiently glycosylated by *Cj*PglB in the cell-free environment.

We also investigated YebF-RNase $A^{H12A/S32D}$ glycosylation in two alternative environments: IVG and *in vivo* (Figure 1). In the case of the IVG environment, a minimally reconstituted glycosylation reaction was performed using solvent extracted *Cj*LLOs, membrane purified *Cj*PglB, and purified YebF-RNase $A^{H12A/S32D}$ acceptor protein. Because the acceptor protein was provided in its completely folded conformation, this environment allowed determination of whether the glycosylation site was accessible to the OST in the context of an already folded acceptor protein. Consistent with previous reports,[19,21] purified YebF-RNase $A^{H12A/S32D}$ was not able to be glycosylated by *Cj*PglB (Figure 2c). In the case of the *in vivo* environment, intracellular expression of YebF-RNase $A^{H12A/S32D}$ was performed using glycocompetent *E. coli* CLM24 cells coexpressing plasmid-encoded copies of *Cj*PglB and the enzymes for *Cj*LLO biosynthesis. In these cells, the acceptor protein is translocated into the periplasm by the SecYEG machinery and subsequently folds; hence, this environment provides an opportunity for *Cj*PglB-mediated glycosylation to proceed both co- and post-translocationally. In line with previous findings,[21,22] YebF-RNase $A^{H12A/S32D}$ was efficiently glycosylated in living cells that co-expressed *Cj*PglB, but not in cells possessing a catalytically inactivated OST (Figure 2c). Given that folded RNase A is not a viable substrate for *Cj*PglB, we concluded that *in vivo* modification of RNase A must involve increased accessibility of the N34 site to *Cj*PglB through either co-translocational glycosylation or post-translocational glycosylation of a partially unfolded structure. Moreover, because the efficiency and levels of glycosylation observed for the *in vivo* and CFGpS systems were virtually identical (Figure 2c), it appears that the CFGpS environment must also involve a mechanism for increasing accessibility of the N34 site to the OST.

Efficient RNase A Glycosylation in CFGpS Does Not Require Translocation but Occurs Prior To Folding. Next, we sought to determine the factors that contributed to the high glycosylation efficiency of the structured domain in YebF-RNase $A^{S32D/H12A}$ in CFGpS. We first investigated whether translocation contributed to the glycosylation of YebF-RNase $A^{S32D/H12A}$ in CFGpS. We speculated that membrane vesicles in the CFGpS environment, which are known to be highly enriched with glycosylation and translocation machinery,[12] might contain active SecYEG translocases that could recognize the Sec-dependent signal peptide at the N-terminus of YebF-RNase $A^{S32D/H12A}$ and promote its translocation into the vesicle lumen. Such internalization into vesicles would provide an opportunity for co-translocational glycosylation analogous to the *in vivo* system. It should be noted that similar co-translocational glycosylation of nascent chains is carried out in eukaryotic CFPS systems supplemented with microsomes, whereby glycoproteins become glycosylated during active transport into the lumen of microsomal vesicles.[35] To test this hypothesis, plasmid pJL1-RNase $A^{S32D/H12A}$ was constructed with the YebF secretion domain removed and the resulting plasmid was used in a CFGpS reaction. Following immunoblotting, we observed strong glycosylation of RNase $A^{S32D/H12A}$ with an efficiency that was nearly identical to that observed for the YebF-fused version (Figure 3a compared to Figure 2b, respectively). We also saw no effect on glycosylation efficiency using CFPS lysates lacking either or both of the flippases, namely *C. jejuni* PglK and *E. coli* WzxE, which are actively expressed from the pMW07-pglΔB plasmid and the CLM24 genome, respectively (Figure S2). This result indicates that the distribution of LLOs on the available vesicle surfaces in CFGpS are likely not a driving factor in glycosylation efficiency. Moreover, because the secretion domain and flippases were not required for glycosylation of RNase $A^{S32D/H12A}$, we conclude that a co-translocational glycosylation mechanism is likely not contributing to the ability of *Cj*PglB to glycosylate structured protein domains in CFGpS.

We next investigated whether access to the structured domain occurred prior to folding, either concomitantly with translation (co-translationally) or before folding was completed (pre-folding), or instead occurred after folding was completed (post-folding). Each of these mechanisms was plausible due to the potential involvement of factors in the CFGpS reaction environment, such as chaperones, detergents, lipids, or unfoldases, that could promote partial unfolding or destabilization of folded RNase A to expose its glycosylation site. We compared two different CFGpS reactions: one where plasmid DNA encoding YebF-RNase $A^{S32D/H12A}$ was added and the other where separately prepared YebF-RNase $A^{S32D/H12A}$ protein was supplemented directly, such that the reaction only involved glycosylating an already translated and folded substrate. As seen above, CFGpS primed with plasmid DNA gave rise to efficient glycosylation of YebF-RNase $A^{S32D/H12A}$ that was transcribed and translated *in situ* (Figure 3b). In contrast, the reaction supplemented with purified YebF-RNase $A^{S32D/H12A}$ resulted in barely detectable glycosylation. Taken together, these results suggest that the ability of *Cj*PglB to glycosylate the structured domain in CFGpS-expressed RNase A depends heavily on active translation and/or folding in the

https://doi.org/10.1021/acssynbio.5c00229
ACS Synth. Biol. 2025, 14, 2354−2367

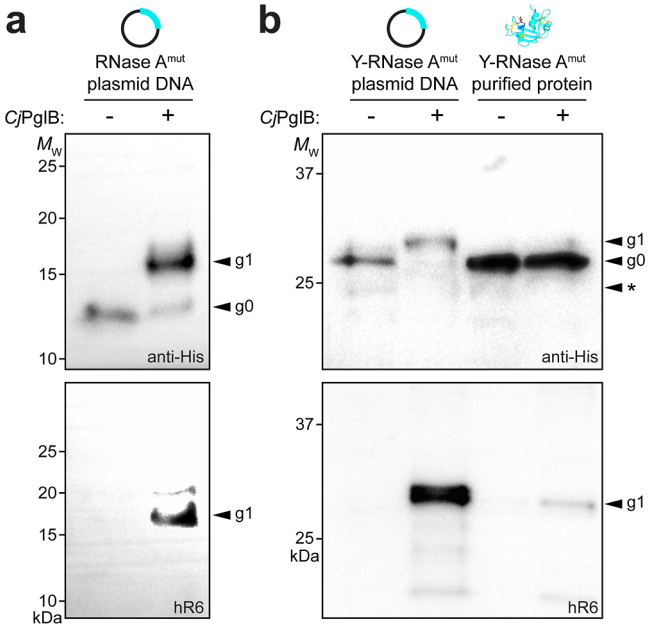

Figure 3. Determinants of RNase A glycosylation in CFGpS. (a) Immunoblot analysis of RNase $A^{H12A/S32D}$ produced in CFGpS S12 lysates enriched with *Cj*LLOs, with (+) or without (−) *Cj*PglB. (b) Immunoblot analysis of (left) YebF-RNase $A^{H12A/S32D}$ produced in CFGpS S12 lysates enriched with *Cj*LLOs, with (+) or without (−) *Cj*PglB and (right) aglycosylated YebF-RNase $A^{H12A/S32D}$ purified from BL21(DE3) and subsequently added to CFGpS S12 lysates enriched with *Cj*LLOs, with (+) or without (−) *Cj*PglB. All blots were probed with either polyhistidine epitope tag-specific antibody (anti-His) to detect the C-terminal 6x-His tag on YebF-RNase $A^{H12A/S32D}$ or RNase $A^{H12A/S32D}$ and separately with antiglycan serum (hR6) to detect the *C. jejuni* heptasaccharide glycan. Molecular weight (M_W) markers are indicated on the left. The g0 and g1 arrows indicate aglycosylated and monoglycosylated acceptor proteins, respectively. Blots are representative of biological replicates (n = 3).

reaction environment, with only a slight contribution from post-translational unfolding/destabilization.

CFGpS Supports Glycosylation of Sequon in Structured Domain of Human Fc. To determine whether CFGpS could glycosylate additional sequons that occur in the structured regions of a protein, we investigated glycosylation of the Fc region of human IgG. The homodimeric Fc region consists of two N-terminal C_H2 domains and two C-terminal C_H3 domains. In eukaryotes, *N*-linked glycans are thought to be predominantly added co-translationally at a highly conserved N297 glycosylation site within the C'E loop of each C_H2 domain (Figure 4a), with glycan addition occurring soon after the acceptor site passes through the membrane and enters the lumen of the ER.[36] Such a co-translational mechanism is required because aglycosylated, completely folded heavy chains cannot be glycosylated after release from the ribosome presumably due to rapid intramolecular folding (i.e., secondary and tertiary structure) and/or intermolecular assembly (i.e., quaternary structure) that renders the acceptor site unavailable to the OST, as suggested by preliminary modeling (Figure S3).[36] Indeed, C_H2 domains, which harbor the conserved ^{295}QYNST^{299} sequon, are in much closer proximity and thus adopt a more closed orientation in aglycosylated dimeric Fc fragments versus their glycosylated counterparts[37,38] (Figure 4a), which might limit solvent accessibility of the sequon.

To investigate Fc glycosylation across all three environments (CFGpS, IVG, and *in vivo*), we created a synthetic construct encoding the entire Fc region (C_H2−C_H3) plus the hinge region derived from human IgG1 with a recoded bacterial sequon, ^{295}DQNAT^{299}, in place of the native ^{295}QYNST^{299} motif. We included the hinge region to enable authentic dimerization of the C_H2−C_H3 chains[39] and used a DQNAT motif because human Fc fragments harboring this mutated sequon can be glycosylated by PglB homologues in glycocompetent *E. coli* cells.[22,40−42] Moreover, because Fc glycosylation in these studies was more efficiently accomplished with PglB homologues from *Desulfovibrio* spp. versus *Campylobacter* spp., due in part to their more eukaryotic-like catalytic pocket,[41,42] we opted to use *Desulfovibrio marinus* PglB (*Dm*PglB) as the OST in all our Fc glycosylation experiments. Lastly, we used a modified bacterial glycan, $GalNAc_5GlcNAc$ (Figure 4b) because it is a potential starting point for existing chemoenzymatic remodeling methods that could yield a eukaryotic complex-type glycan such as the asialo afucosylated $Gal_2GlcNAc_2Man_3GlcNAc_2$ glycan known as G2.[43] For *in vivo* glycosylation, the hinge-Fc^{DQNAT} construct was expressed in glycocompetent CLM24 cells along with plasmid-encoded copies of *Dm*PglB and the enzymes for biosynthesis of $GalNAc_5GlcNAc$ LLOs. In line with earlier reports of human Fc glycosylation in *E. coli*,[22,40,44] we observed strong glycosylation as evidenced by the appearance of g1 and g2 glycoforms in the anti-IgG and antiglycan blots, which corresponded to hemi and fully-glycosylated hinge-Fc^{DQNAT} products, respectively (Figure 4c). As expected, this glycosylation depended on co-expression of a functional OST. In contrast, when aglycosylated hinge-Fc^{DQNAT} was purified from CLM24 cells and subjected to IVG in the presence of membrane purified *Dm*PglB and solvent-extracted LLOs bearing the $GalNAc_5GlcNAc$ glycan, no detectable glycosylation was observed (Figure 4c). Collectively, these results confirmed that the Fc sequon is inaccessible to *Dm*PglB in the folded and assembled structure and that *in vivo* glycosylation of this site likely involves a co-translocational mechanism, akin to RNase A.

We next determined whether the Fc glycosylation site was accessible to *Dm*PglB in the CFGpS environment. For this experiment, we modified the workflow that was used above for RNase A because of the more complicated folding and assembly of the hinge-Fc dimer. Specifically, we implemented an extract mixing strategy (Figure 4b) that was inspired by a previous cell-free metabolic engineering framework whereby multiple crude lysates were mixed to construct a full biosynthetic pathway.[45] This involved preparing a first extract for supporting disulfide bond formation (S−S extract). We started with extract from SHuffle T7 Express, which is known to enable production of proteins with disulfide bonds. However, because the hinge-Fc requires a more complicated arrangement of disulfide bonds for soluble expression, folding, and assembly into a dimer,[46] we supplemented this extract with purified disulfide bond isomerase DsbC and prolyl isomerase FkpA, both of which were previously identified as important positive effectors of full-length IgG folding in CFPS.[47] The second and third extracts were derived from CLM24 expressing *Dm*PglB and the enzymes for biosynthesis of $GalNAc_5GlcNAc$ LLOs, respectively, yielding OST and LLO extracts that were selectively enriched with the requisite glycosylation machinery. To assemble a complete biosynthetic pathway for cell-free Fc expression, folding, and glycosylation,

https://doi.org/10.1021/acssynbio.5c00229
ACS Synth. Biol. 2025, 14, 2354−2367

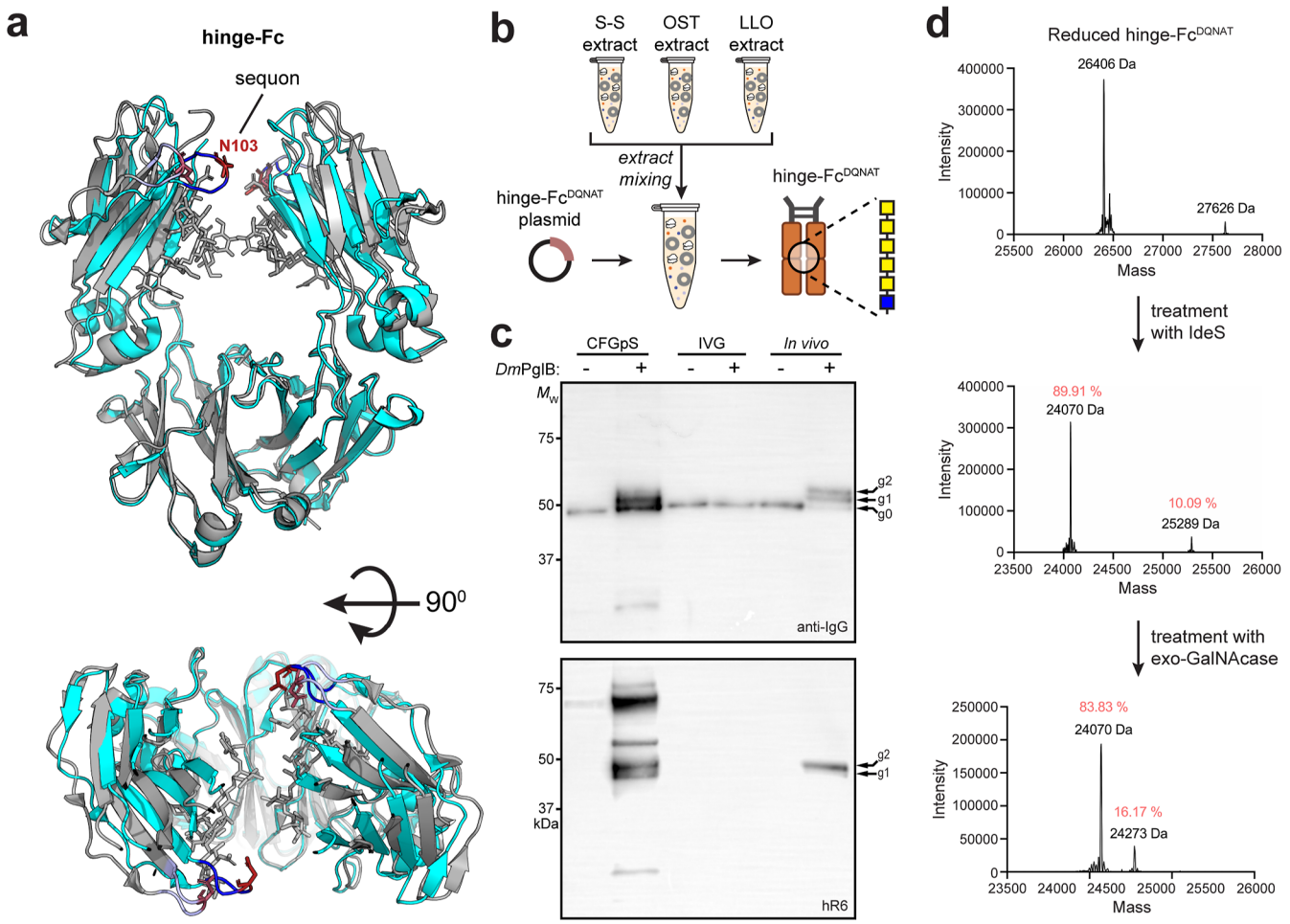

Figure 4. Efficient glycosylation of acceptor site in hinge-Fc using CFGpS. (a) Comparison of glycosylated and aglycosylated Fc structures (lacking hinge domain). Glycosylated Fc (PDB ID: 3AVE; grey) is compared with the A,B dimer of aglycosylated Fc (PDB ID: 3S7G; cyan). P329 distances (measured from Cαs) for 3AVE and 3S7G are 25.1 Å and 18.5 Å, respectively.[37] (b) CFGpS expression and glycosylation of hinge-Fc^{DQNAT} was performed by adding the plasmid pJL1-human-Fc^{DQNAT} to a reaction mixture of separate S12 lysates prepared from SHuffle T7 express (S−S extract), CLM24 expressing *Dm*PglB (OST extract), and CLM24 expressing enzymes encoding GalNAc$_5$GlcNAc LLO biosynthesis enzymes (LLO extract). (c) Non-reducing immunoblot analysis of protein A-purified hinge-Fc^{DQNAT} proteins generated in the CFGpS, IVG, and *in vivo* systems. Hinge-Fc^{DQNAT} was produced in CFGpS S12 lysates enriched with GalNAc$_5$GlcNAc LLOs, with (+) or without (−) *Dm*PglB, and with (+) or without (−) the acceptor protein expression plasmid, pJL1-hinge-Fc^{DQNAT}. IVG was performed using aglycosylated hinge-Fc^{DQNAT} purified from CLM24 cells carrying plasmid pTrc99S-ssDsbA-hinge-Fc^{DQNAT}, solvent extracted GalNAc$_5$GlcNAc LLOs, and membrane purified *Dm*PglB. *In vivo* glycosylation was performed using CLM24 cells carrying plasmid pTrc99S-ssDsbA-hinge-Fc^{DQNAT}, pMW07-pglΔBICDEF for producing GalNAc$_5$GlcNAc LLOs, and either pMAF10-*Dm*PglB for OST expression (+) or an analogous plasmid that expresses *Dm*PglB^{mut} (−), a catalytically inactive mutant of *Dm*PglB described in Sotomayor et al.[44] All blots were probed with either human Fc-specific antibody (anti-IgG) to detect hinge-Fc^{DQNAT} or antiglycan serum (hR6) that detects the GalNAc$_5$GlcNAc glycan. Molecular weight (M_W) markers are indicated on the left. The g0, g1, and g2 arrows indicate aglycosylated, mono-, and diglycosylated acceptor proteins, respectively. Blots are representative of biological replicates (n = 3). (d) LC-ESI-MS analysis of dithiothreitol (DTT) reduced hinge-Fc^{DQNAT} (top panel), which was subsequently treated with IdeS (middle panel), a bacterial protease that cleaves human IgG at a site just below the hinge region, and exo-GalNAcase (bottom panel), a bacterial exoglycosidase that hydrolyzes terminal, non-reducing α-GalNAc residues from *N*-glycans attached to proteins. Signal at m/z = 24,070 corresponds to monomeric aglycosylated hinge-Fc^{DQNAT}, signal at m/z = 25,289 corresponds to GalNAc$_5$GlcNAc-hinge-Fc^{DQNAT}, and signal at m/z = 24,273 corresponds to GlcNAc-hinge-Fc^{DQNAT}.

the three separately prepared extracts were mixed at a volumetric ratio of 1:2:1 (S−S/LLO/OST) and the reaction mixture was subsequently primed with plasmid pJL1-hinge-Fc^{DQNAT}. Immunoblot analysis of the resulting products revealed the formation of the same g2 and g1 glycoforms that were detected in the *in vivo* environment, albeit with less efficient glycosylation overall (Figure 4c). The blot also showed efficient disulfide bond-mediated assembly of the Fc to the expected size of 50 kDa with two potential glycosylation sites. To unequivocally confirm glycosylation of the hinge-Fc^{DQNAT}, the protein was purified from the CFGpS reaction using protein A affinity chromatography (Figure S4) and analyzed by mass spectrometry. LC-ESI-MS analysis of the protein A-purified hinge-Fc^{DQNAT} as well as its IdeS-treated derivative revealed that the reduced monomer was ∼10−20% glycosylated with the expected HexNAc$_6$ glycoform, which consisted of five GalNAc residues as confirmed by exo-α-*N*-acetylgalactosaminidase (exo-GalNAcase) treatment that removed all but one HexNAc (Figure 4d). LC−MS/MS analysis of the purified hinge-Fc^{DQNAT} following denaturation, alkylation, and tryptic digestion identified a peptide (^{79}EEDQNATYR) modified with the HexNAc$_6$ glycoform,

https://doi.org/10.1021/acssynbio.5c00229
ACS Synth. Biol. 2025, 14, 2354−2367

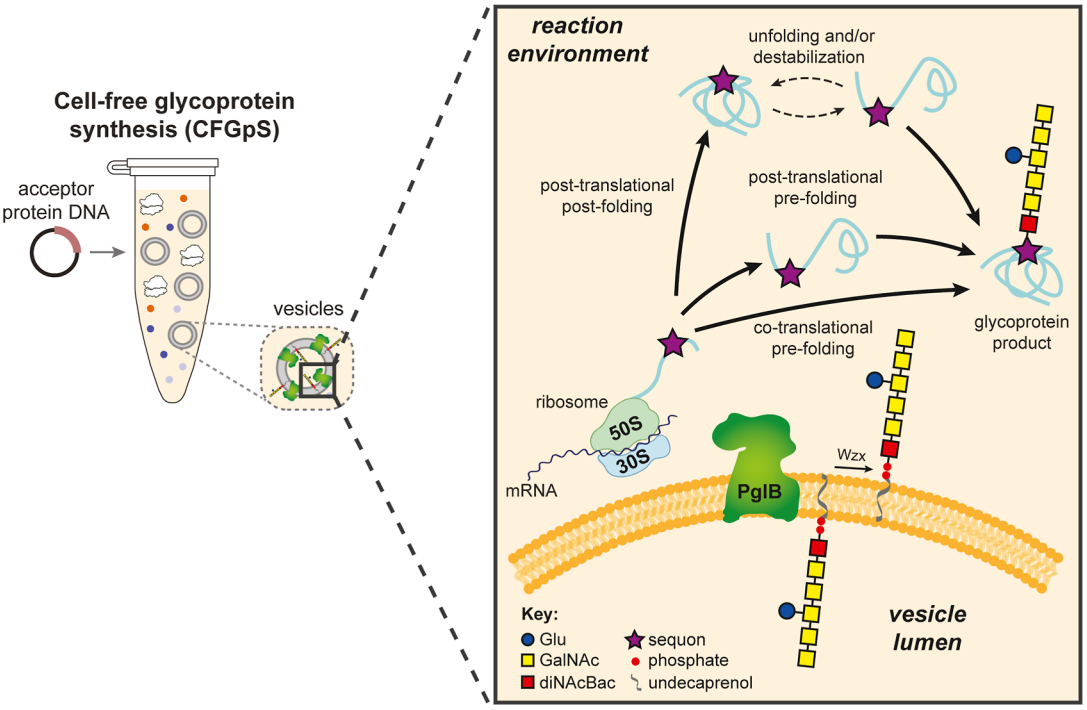

Figure 5. Proposed model for *N*-glycosylation of structured protein domains in CFGpS. Synthesis of an acceptor protein from acceptor protein mRNA results in a nascent polypeptide that emerges from the exit tunnel of the ribosome. The polypeptide is predominantly glycosylated either as it is being synthesized (co-translational, pre-folding) or after release from the ribosome, but prior to assuming its final folded confirmation (post-translational, post-folding). A negligible amount of fully folded acceptor protein may be temporarily unfolded or destabilized by the reaction environment and glycosylated (post-translational, post-folding). Because the *N*-glycosylation components, including the OST and LLOs, are membrane associated, this process likely occurs at or near the interface of the vesicles and reaction environment.

thereby confirming the identity and location of glycan attachment to the expected asparagine residue within the Fc glycosylation site (Figure S5). Importantly, the ability of the mixed CFGpS extract to support glycosylation of the Fc sequon, which was inaccessible to *Dm*PglB when the Fc fragment was already folded and assembled, further suggests that co-translational glycosylation is active in this environment.

DISCUSSION

Here, we demonstrate the ability of the CFGpS reaction environment to support efficient glycosylation of two eukaryotic glycoproteins, namely bovine RNase A and human hinge-Fc. Importantly, CFGpS-mediated glycosylation efficiency was comparable with that achieved *in vivo* following expression and translocation to the periplasm of glycocompetent *E. coli* cells. This discovery is significant because completely folded RNase A and hinge-Fc were refractory to glycosylation, as we demonstrated in IVG reactions supplied with already-folded RNase A and hinge-Fc proteins. These results were consistent with previous observations that fully folded conformations of bovine RNase A and *C. jejuni* PEB3 were barely glycosylated *in vitro*, with higher levels of glycosylation only becoming possible when the proteins were chemically unfolded or partially destabilized, respectively.[19,20] Based on these observations, we concluded that the ability of the CFGpS and *in vivo* glycosylation systems to glycosylate acceptor sites in challenging regions (i.e., structured or solvent-inaccessible) must involve glycan installation by the OST prior to the proteins achieving a fully folded conformation.

In CFGpS, glycosylation of such challenging sequons was observed to depend significantly on protein translation but not on membrane translocation. The dependence on translation allows us to rule out the possibility that factors such as chaperones and/or unfoldases in the CFGpS reaction post-translationally destabilize or partially unfold RNase A to meaningfully reveal the glycosylation site. Furthermore, the lack of any significant contribution from translocation indicates that the mechanism by which these domains are glycosylated in CFGpS must differ from how such domains are glycosylated in higher eukaryotes. Specifically, in mammalian cells structured domains can be glycosylated prior to folding by a co-translocational mechanism, whereby nascent proteins undergoing active translocation to the lumen of the rough endoplasmic reticulum (RER) are concomitantly glycosylated by a hetero-oligomeric OST complex that includes the STT3A isoform of the catalytic subunit.[48] The coordination of translocation and glycosylation is facilitated by direct interactions between subunits of the general secretion (Sec) translocation machinery and the OST subunits.[49] At present, it is not known whether *N*-glycosylation and protein translocation are similarly coupled in bacteria as they are in higher eukaryotes and there is no evidence of a direct interaction between the translocation machinery and OST. Therefore, in the context of our *E. coli* based CFGpS system, we favor a model whereby the challenging sequons in RNase A and hinge-Fc are glycosylated either while the nascent polypeptide is still being synthesized by the ribosome (co-translational) or shortly after the nascent chain exits the ribosome but before it has reached its final folded confirmation (pre-folding) (Figure 5). A similar mechanism likely exists in yeast and glycocompetent *E. coli* where tight coupling between the Sec translocase and the OST is absent[19,20,50] yet both are able to efficiently glycosylate RNase A and IgG-Fc domains.[21,22,44,51,52]

https://doi.org/10.1021/acssynbio.5c00229
ACS Synth. Biol. 2025, 14, 2354−2367

While the precise mechanism and timing for *N*-glycan installation in CFGpS remains unknown, it is noteworthy that a similar crude extract-based, cell-free system derived from *E. coli* exhibits a translation elongation rate of 1.5−2 amino acids per second, which is ∼10-fold and ∼3-fold slower than the translation rates in living *E. coli* cells and mammalian cells, respectively.[53] This slower rate might provide an opportunity for the ribosome-tethered nascent chain to be glycosylated in an extended conformation as it emerges from the exit tunnel, but before upstream sequences involved in folding emerge. Such a ribosome-centric mechanism would be biologically feasible given prior evidence that *Cj*PglB is able to install *N*-glycans onto ribosome-stalled polypeptides in CFGpS.[54] It is also possible that a chaperone or other accessory factor might engage with newly synthesized proteins in a manner that increases accessibility to glycosylation sites in structured regions, for example, by slowing formation of the native conformation. Indeed, the exit tunnel region of the ribosome is well established as a hub for interactions that occur between nascent polypeptides and components that guide their fate such as the molecular chaperone trigger factor (TF).[55] It should be noted that even though protein translocation was found to be dispensable for glycosylation of the RNase A sequon, we cannot rule out the possibility that some protein substrates are translocated and subsequently glycosylated in the lumen of vesicles known to be present in CFGpS lysates derived from *E. coli*.[12] Moreover, the use of high-pressure homogenization for preparing cell-free extracts is known to form a mixture of right-side-out (i.e., the same topology as the parental cells) and inside-out or inverted membrane vesicles,[56−58] with the latter providing functional translocation machinery that would be accessible to newly translated proteins and enable their transport into the vesicle lumen.[59]

In conclusion, we have provided strong evidence that the CFGpS environment can support glycosylation of challenging sequons that are in structured or solvent-inaccessible regions of a substrate protein. Our findings suggest that *N*-glycosylation in CFGpS is a temporally and spatially coordinated process that resembles archetypical glycosylation in living cells but appears to diverge in several important ways. These findings also highlight how the open reaction environment of CFGpS allows for simplified investigation of the glycosylation mechanism in a cell-like environment that would otherwise be challenging to perform *in vivo*. Moreover, while CFGpS and IVG may appear conceptually analogous, the ability to glycosylate sequons in structured protein regions is an emergent property of CFGpS that arises from the co-activation of transcription/translation and glycosylation, which is absent in IVG reactions. In terms of practical utility, the work presented here is the first demonstration of IgG Fc glycosylation in a cell-free reaction and is significant given the demonstration that Fc fragments bearing precise glycan structures are promising intravenous immunoglobulin (IVIG) alternatives for the treatment of a wide variety of autoimmune disorders.[60] While the glycosylation efficiency reported here was only ∼10−20%, we note that similarly low glycosylation efficiency has also been reported for bacterial cell-based glycosylation of IgG Fc domains, making this an area for improvement in the future. For example, increased glycosylation efficiency might be achieved by tuning the rates of ribosomal translation and folding/unfolding of protein substrates using strategies such as optimization of 5′ untranslated regions (UTRs), strategic incorporation of rare codons, and supplementation of molecular chaperones. We also note that the *N*-glycans attached here were bacterial in origin; however, conversion of the $GalNAc_5GlcNAc$ structure to a homogeneous, complex-type human *N*-glycan could be imagined by integrating our CFGpS platform with chemoenzymatic glycan remodeling strategies.[43,44] Looking ahead, it will be important to further disentangle pathway dynamics and identify additional accessory factors, if any exist, that underlie CFGpS-mediated glycosylation of antibody Fc domains. Such studies would not only deepen our understanding of this important life process but could also enable platform optimization that will be required for portable, efficient, and scalable biomanufacturing of therapeutically important proteins with customized glycosylation including monoclonal antibodies and Fc-fusion proteins.[11,14,16] If completed, this work could improve their overall effectiveness as therapeutics while enabling both artificial intelligence driven high-throughput protein design campaigns and worldwide, on-demand access to these life-saving medicines.

MATERIAL AND METHODS

Bacterial Strains. *E. coli* strain DH5α was used for all plasmid construction in this study. *E. coli* strain BL21(DE3) (Novagen) was used for recombinant expression and purification of PglB enzymes and for periplasmic expression of RNase A variants used for IVG experiments. *E. coli* strain SHuffle T7 Express (NEB)[31] was used to produce lysate for CFGpS experiments. *E. coli* strain CLM24[61] was used for the preparation of lysates enriched with glycosylation components, expression of glycans that were subsequently solvent-extracted, and periplasmic expression of human hinge-Fc^{DQNAT}.

Plasmid Construction. For expression of YebF-RNase A in CFGpS, plasmid pJL1-YebF-RNase $A^{S32D/H12A}$ was constructed by PCR amplifying the YebF-RNase A^{S32D} coding sequence from pTrc99S-YebF-RNase A^{S32D} that was generated previously[21] and cloning it into plasmid pJL1, a pET-based vector used for CFPS,[62] using Gibson assembly. The inactivating H12A mutation was introduced into the YebF-RNase A^{S32D} coding sequence using site-directed mutagenesis (SDM). For expression of YebF-RNase A in cells, plasmid pTrc99S-YebF-$RNase^{S32D/H12A}$ was generated via SDM of plasmid pTrc99S-YebF-RNase A^{S32D}. Plasmid pJL1-RNase $A^{S32D/H12A}$ was generated by PCR amplifying only the RNase $A^{S32D/H12A}$ coding sequence from pJL1-YebF-RNase $A^{S32D/H12A}$ and recircularizing the plasmid using Gibson assembly. Plasmid pJL1-RNase A^{S32D} was generated by PCR amplifying only the RNase A^{S32D} coding sequence from pJL1-YebF-RNase A^{S32D} and recircularizing the plasmid using Gibson assembly. For expression of hinge-Fc in cells, plasmid pTrc99S-spDsbA-hinge-Fc^{DQNAT} was created by adding the hinge sequence EPKSCDKTHTCPPCP between the *E. coli* DsbA signal peptide and the human IgG1 Fc domain in pTrc-spDsbA-Fc^{DQNAT}.[40] For expression of hinge-Fc in CFGpS, plasmid pJL1-hinge-Fc^{DQNAT} was generated by cloning the coding sequence for the hinge-Fc^{DQNAT} region from pTrc99-spDsbA-hinge-Fc^{DQNAT} into the pJL1 backbone using Gibson assembly. For expression of *Cj*PglB, $CjPglB^{mut}$, *Dm*PglB and $DmPglB^{mut}$ in cells, plasmids pMAF10,[61] pMAF10-$CjPglB^{mut}$[27] and pMAF10-*Dm*PglB,[44] and pMAF10-$DmPglB^{mut}$[44] were used. For expression of OSTs in CFGpS, we used pSF-*Cj*PglB that was described previously[42] and constructed pSF-*Dm*PglB by cloning the coding sequence from pMAF10-*Dm*PglB into the pSF backbone using Gibson assembly. To prepare OSTs for

https://doi.org/10.1021/acssynbio.5c00229
ACS Synth. Biol. 2025, 14, 2354−2367

IVG, we used pSN18-*Cj*PglB[19] and pSF-*Dm*PglB-10xHis[44] for expressing and purifying *Cj*PglB and *Dm*PglB, respectively. For biosynthesis of the $GalNAc_5$(Glc)diNAcBac glycan, plasmid pMW07-pglΔB was used[27] while biosynthesis of the $GalNAc_5$GlcNAc glycan was carried out with plasmid pMW07-pglΔBICDEF.[44] All plasmids were confirmed by DNA sequencing at Eurofins Genomics Inc. and Plasmidsaurus Inc.

Protein Expression and Purification. For IVG reactions, *Cj*PglB and *Dm*PglB were purified from cell membranes as described previously.[44,63] Purification of aglycosylated YebF-RNase$^{S32D/H12A}$ was prepared for IVG reactions as follows. First, a colony of BL21(DE3) cells carrying plasmid pTrc99S-YebF-RNase$^{S32D/H12A}$ was inoculated in 20 mL of Luria−Bertani (LB) media supplemented with 50 μg/mL spectinomycin (Spe) in a 125-mL culture flask and grown for 16 h at 37 °C with shaking at 250 rpm. Then, 20 mL of saturated starter culture was used to inoculate 1 L of LB in a 2.8-L culture flask supplemented with 50 μg/mL Spe. This culture was subsequently incubated at 37 °C with shaking at 250 rpm until the optical density at 600 nm (OD_{600}) of the culture reached ∼0.7, at which point protein expression was induced with 1 mM isopropyl-β-D-thiogalactoside (IPTG). Protein expression was allowed to proceed for 16−20 h at 30 °C with shaking at 250 rpm, after which cells were harvested via centrifugation by spinning at 8000*g* and 4 °C for 15 min. Pellets were resuspended with 10 mL of desalting buffer (50 mM NaH_2PO_4, 300 mM NaCl, pH 8, sterile filtered) per 1 g of pellet and lysed using an Emulsiflex-C5 High Pressure Homogenizer (Avestin) at 16,000−18,000 psi for approximately 8 min. The insoluble fraction was pelleted by spinning the lysate at 18,000*g* and 4 °C for 25 min. A total of 500 μL of HisPur Ni-NTA resin (ThermoFisher) was equilibrated with 10 mM imidazole desalting buffer (10 mM imidazole, 50 mM NaH_2PO_4, 300 mM NaCl, pH 8, sterile filtered) and then incubated with the soluble lysate at 4 °C for 1 h with end-over-end mixing. An Econo-Pac Chromatography Column (Bio-Rad) was prepared by flowing 1 mL of autoclaved water through the column followed by 1 mL of 10 mM imidazole desalting buffer. The soluble lysate plus resin mixture was subsequently flowed through the column, collected, and re-run through the column. The column was subsequently washed 3 times with 1 mL of 20 mM imidazole desalting buffer (20 mM imidazole, 50 mM NaH_2PO_4, 300 mM NaCl, pH 8, sterile filtered). The purified product was eluted twice, each time using a 1-min incubation with 1 mL of 300 mM imidazole desalting buffer (300 mM imidazole, 50 mM NaH_2PO_4, 300 mM NaCl, pH 8, sterile filtered). The resulting product was buffer exchanged into 1× phosphate-buffered saline (PBS) using a PD-10 column (Cytiva) and stored at 4 °C until use.

Purified hinge-Fc^{DQNAT} for IVG reactions was prepared as follows. First, 10 mL of LB supplemented with 50 μg/mL Spe was inoculated with a colony of CLM24 carrying pTrc99S-spDsbA-hinge-Fc^{DQNAT} and incubated for 16−20 h at 37 °C with shaking at 250 rpm. Next, two 500-mL shake flasks containing 100 mL of LB supplemented with 50 μg/mL Spe were each inoculated with 1 mL of saturated starter culture and incubated at 37 °C with shaking at 250 rpm. When the OD_{600} reached ∼0.7, protein expression was induced with 0.1 mM IPTG. The incubation temperature was changed to 30 °C and protein expression was allowed to proceed for 16−20 h. Following induction, the cultures were combined and centrifuged for 10 min at 10,000*g* and 4 °C. Harvested cells were resuspended in a volume of PBS, 1× HALT protease inhibitor cocktail (EDTA free; ThermoFisher) and 5 mM EDTA equal to one-tenth of the original culture volume. Cells were ruptured by passage through an Emulsiflex-C5 High Pressure Homogenizer (Avestin) at 16,000−18,000 psi. The cell lysate was then clarified by centrifugation for 30 min at 18,000*g* and 4 °C. At the same time, 1 mL of MabSelect SuRe protein A resin (Cytiva) slurry was equilibrated with 10 mL of equilibration buffer (0.1 M NaH_2PO_4, 0.15 M NaCl, pH 8, sterile filtered). The cell lysate and equilibration buffer were mixed in a 1:1 ratio by volume and flowed through the column, after which the column was washed with 20 mL of equilibration buffer. Tubes for collecting the elution fraction were filled with 100 μL neutralizing buffer (1 M Tris-base, pH 9, sterile filtered) each. Elution buffer (0.15 M glycine, pH 2.2, sterile filtered) was subsequently added in 1-mL fractions to the column until no more protein was eluted (approximately 3 fractions total). Fractions containing protein were combined and exchanged into PBS using 5 mL Zeba Spin Desalting Columns (ThermoFisher). Protein concentration was quantified by absorbance at 280 nm using a NanoDrop 1000 (ThermoFisher).

For hinge-Fc^{DQNAT} glycosylation in CFGpS, purification of *E. coli* DsbC and FkpA was performed as described.[64] Briefly, *E. coli* BL21(DE3) carrying a pET28a plasmid encoding either FkpA or DsbC proteins was streaked on a plate. Colonies were picked and grown in 1-L shake flasks of Terrific Broth at 37 °C at 250 rpm. After induction at $OD_{600} \approx 0.6-1.0$, the cultures were shifted to 20 °C overnight. The cells were pelleted and resuspended with 4 mL of Buffer W (IBA) per gram of wet cell weight followed by lysis using a C3 homogenizer (Avestin). The lysate was then clarified by centrifugation and loaded onto a column with Streptacin-XT 4Flow resin (IBA) using PBS for 10 column volumes (CV) of washing and PBS with 50 mM biotin for elution. The proteins were dialyzed into PBS with 5% (v/v) glycerol . For DsbC dialysis, the buffer was additionally supplemented with 200 μM of dithiothreitol (DTT). After overnight dialysis, the proteins were concentrated to 515 μM for DsbC and 1016 μM for FkpA (determined by Nanodrop 1000 absorbance at 280 nm with theoretical extinction coefficient), flash frozen, and stored at −80 °C until use.

Cell-Based Expression and Glycosylation. To express and glycosylate YebF-RNase A$^{S32D/H12A}$ in living *E. coli* cells, a single colony of CLM24 carrying pMW07-pglΔB, pMAF10-*Cj*PglB, and pTrc99S-YebF-RNase A$^{H12A/S32D}$ was used to inoculate 5 mL of LB supplemented with 34 μg/mL chloramphenicol (Cm), 100 μg/mL trimethoprim (Tmp), and 50 μg/mL Spe. Cells were grown for 16 h at 37 °C with shaking at 250 rpm. Then, 4 mL of saturated overnight culture was used to inoculate 100 mL of LB with appropriate antibiotics and grown at 37 °C with shaking at 250 rpm. When the OD_{600} of the culture reached ∼0.8, protein expression was induced by adding 0.1 IPTG and 0.2% (w/v) L-arabinose and induced cells were incubated for 16 h at 30 °C with shaking at 250 rpm. Harvest and purification were performed as described above for aglycosylated YebF-RNase A$^{S32D/H12A}$.

To express and glycosylate hinge-Fc^{DQNAT} in living *E. coli* cells, a single colony of CLM24 carrying pMW07-pglΔBICDEF, pMAF10-*Dm*PglB, and pTrc99S-ssDsbA-hinge-Fc^{DQNAT} was used to inoculate 2 mL of LB supplemented with 0.2% (w/v) glucose, 34 μg/mL Cm, 50 μg/mL Spe, and 100 μg/mL Tmp and grown overnight (16 h) at 37 °C and 250 rpm. Next,

https://doi.org/10.1021/acssynbio.5c00229
ACS Synth. Biol. 2025, 14, 2354−2367

200 μL of saturated starter culture was used to inoculate 5 mL of LB supplemented with appropriate antibiotics, after which cells were incubated at 37 °C with shaking at 250 rpm. When the OD_{600} reached ∼1.4, protein expression and glycosylation was induced by adding 0.1 mM IPTG and 0.2% (w/v) L-arabinose. Induced cultures were subsequently incubated at 30 °C and 250 rpm for 16 h. Periplasmic extracts were derived from *E. coli* cultures as follows. First, cells were harvested following induction and normalized to an $OD_{600} \approx 2$. The normalized cells were then centrifuged at 6000*g* for 2 min at 4 °C after which the pellets were resuspended in 200 μL of 0.4 M arginine buffer and incubated at 4 °C for 1 h. Next, the samples were centrifuged at 16,000*g* at 4 °C for 1 min and the supernatant was collected as the periplasmic extract. The hinge-Fc^{DQNAT} was purified from the resulting periplasmic extracts using NAb Protein A Plus spin columns (ThermoFisher) according to the manufacturer's instructions, buffer exchanged into PBS, and subsequently stored at 4 °C until further use.

Preparation of Cell-Free Lysates. Preparation of S12 lysates from *E. coli* has been described previously.[12,16,65] Here, SHuffle T7 Express were grown in 1 L of 2 × YTPG (10 g/L yeast extract, 16 g/L tryptone, 5 g/L NaCl, 3.0 g/L KH_2PO_4, 7.0 g/L K_2HPO_4, 8.0 g D-glucose (+), pH 7.4) media at 37 °C with shaking at 250 rpm. Cells were grown to an OD_{600} of ∼3, then harvested by centrifugation at 10,000*g* and 4 °C for 10 min. For enrichment of glycosylation components in the lysate, source strains carrying plasmids encoding glycosylation components were grown at 37 °C in 2xYTP (10 g/yeast extract, 16 g/L tryptone, 5 g/L NaCl, 3.0 g/L KH_2PO_4, 7.0 g/L K_2HPO_4, pH 7.4) with 34 μg/mL Cm or 100 μg/mL Ampicillin (Amp) or both as appropriate. Cells were induced with 0.2% (w/v) L-arabinose at an OD_{600} of ∼0.8, shifted to 30 °C, and harvested at an OD_{600} of ∼3. All subsequent steps were carried out at 4 °C and on ice unless otherwise stated. Pelleted cells were resuspended in 50 mL of S30 buffer (10 mM Tris acetate pH 8.2, 14 mM magnesium acetate, 60 mM potassium acetate). Cells were then washed 3 times by centrifuging the resuspended cells at 10,000*g* for 3 min at 4 °C, pouring off the supernatant, and resuspending in 50 mL of S30 buffer. After the last wash, cells were pelleted at 10,000*g* for 3 min, flash-frozen, and stored at −80 °C. After growth and harvest, cells were thawed and resuspended to homogeneity in 1 mL of S30 buffer per gram of cells. For homogenization, cells were disrupted using an EmulsiFlex-B15 high-pressure homogenizer (Avestin) at ∼22,000 psig with a single pass. The lysate was centrifuged once at 12,000*g* for 10 min and the supernatant collected. Next, the CLM24 source strain lysates were subjected to a 1 h runoff reaction at 37 °C and shaking at 250 rpm in an opaque container. All lysates were then centrifuged at 10,000*g* for 10 min at 4 °C. Supernatants were collected, aliquoted, flash-frozen in liquid nitrogen, and stored at −80 °C.

IVG Reactions. Solvent extraction of lipid-linked sugar donors, namely *Cj*LLOs and $GalNAc_5GlcNAc$ LLOs, was performed according to a previously described protocol.[63] IVG reactions for YebF-RNase $A^{S32D/H12A}$ and hinge-Fc^{DQNAT} were performed as follows. Purified acceptor protein (YebF-RNase $A^{S32D/H12A}$ or hinge-Fc^{DQNAT}) was added at a concentration of 0.02 mg/mL to a reaction with 0.1 mg/mL of purified OST (*Cj*PglB or *Dm*PglB, respectively), and 10% (v/v) LLOs (*Cj*LLOs or $GalNAc_5GlcNAc$ LLOs, respectively) in IVG buffer (10 mM HEPES, pH 7.5, 10 mM MnCl2, and 0.1% (w/v) *n*-dodecyl-*β*-D-maltoside (DDM), sterile filtered). After mixing these components, the reaction was incubated at 30 °C for 16 h.

CFGpS Reactions. CFGpS-based expression and glycosylation of YebF-RNase $A^{S32D/H12A}$ was performed in a two-stage process that was modeled after previously described protocols,[12,16] and the original reaction mixtures previously described.[57,58] All CFGpS reagents were purchased from Sigma-Aldrich unless otherwise specified. In the first stage, 12 mM magnesium glutamate; 10 mM ammonium glutamate (Cayman Chemical); 130 mM potassium glutamate; 1.2 mM ATP; 0.85 mM of GTP, UTP, and CTP; 0.075 mg/mL folinic acid, 0.17 mg/mL *E. coli* tRNA mixture from strain MRE600 (Roche); 0.33 mM nicotinamide adenine dinucleotide (NAD); 0.27 mM coenzyme-A (CoA); 4 mM oxalic acid; 1 mM putrescine; 1.5 mM spermidine; 57 mM HEPES at pH = 7.2; 2 mM each of the 20 standard amino acids; 33 mM phosphoenolpyruvate (Roche); 0.10 mg/mL T7 RNA polymerase (NEB); 4 mM oxidized L-glutathione (GSSG; Amresco); 1 mM reduced L-glutathione (GSH; Alfa Aesar), 13.33 ng/μL plasmid pJL1-YebF-RNase $A^{S32D/H12A}$ prepared using HiSpeed Midiprep kit (Qiagen); and 30% (v/v) of S12 lysate from SHuffle T7 express carrying plasmid pSF-*Cj*PglB for producing *Cj*PglB and plasmid pMW07-pglΔBICDEF for producing the $GalNAc_5GlcNAc$ LLO were combined into a semioxidizing reaction in a thin-film format and incubated for 1 h at 30 °C. Next, in the second stage, glycosylation was initiated by adding 25 mM $MnCl_2$ and 0.1% (w/v) DDM to the reactions which were then incubated for 16 h at 30 °C.

CFGpS-based expression and glycosylation of hinge-Fc^{DQNAT} was performed in a two-stage process that was adapted from a prior protocol.[66] Briefly, the finalized optimal ratio of lysates was determined using a design of experiments approach whereby the titer and glycosylation efficiency of hinge-Fc^{DQNAT} was characterized using SDS-PAGE gel analysis when differing ratios of lysates were used in the CFGpS reactions. For all hinge-Fc^{DQNAT} reactions, each of the three separately prepared extracts were treated with 750 μM iodoacetamide (IAM) in the dark at RT for 30 min immediately prior to preparing the reaction. In the first stage, reactions were assembled in a thin-film format containing 10% (v/v) IAM-treated S12 extract from SHuffle T7 Express; 20% (v/v) IAM-treated S12 extract from CLM24 carrying plasmid pMW07-pglΔBICDEF for producing $GalNAc_5GlcNAc$ LLOs; 10% (v/v) IAM-treated S12 extract from CLM24 carrying pMAF10-*Dm*PglB for producing *Dm*PglB; 4 mM magnesium glutamate; 10 mM ammonium glutamate (Cayman Chemical); 130 mM potassium glutamate; 35 mM sodium pyruvate; 1.2 mM AMP; 0.86 mM of GMP, UMP, and CMP; 2 mM for each of the standard 20 amino acids except for tyrosine which was added at 1 mM; 9.2 mM dibasic potassium phosphate; 5.8 mM monobasic potassium phosphate; 4 mM sodium oxalate; 1 mM putrescine; 1.5 mM spermidine; 4 mM oxidized L-glutathione (GSSG); 1 mM reduced L-glutathione (GSH); 13.33 ng/μL plasmid pJL1-hinge-Fc^{DQNAT} prepared using HiSpeed midiprep (Qiagen); 14 μM purified *E. coli* DsbC; and 50 μM purified *E. coli* FkPa. After mixing all components, reactions were incubated for 30 min at 25 °C in a Thermomixer (Eppendorf). Then, in the second stage glycosylation was initiated by adding 25 mM $MnCl_2$ and 0.1% (w/v) DDM to the reactions, which were then incubated for 16 h at 25 °C.

https://doi.org/10.1021/acssynbio.5c00229
ACS Synth. Biol. 2025, 14, 2354−2367

Purification of CFGpS and IVG Reaction Products. For purification of YebF-RNase $A^{S32D/H12A}$ and RNase $A^{S32D/H12A}$ from the CFGpS reaction, 3 μL of Ni-NTA resin (ThermoFisher) per 1 μL of CFGpS reaction was equilibrated with 10 mM imidazole desalting buffer. The equilibrated resin was mixed with the CFGpS reaction in a 15-mL tube, brought to a total volume of 10 mL with 10 mM imidazole desalting buffer, and incubated with end-overend rotation at 4 °C for at least 2 h. A 10-mL Poly prep Chromatography Column (Bio-Rad) was prepared by flowing 2 mL of ddH_2O followed by 2 mL of 10 mM imidazole desalting buffer through the column. After incubation, the reaction mixture plus resin was flowed through the column twice. The column was then washed twice with 6 CV of 20 mM imidazole desalting buffer and the target protein eluted 4 times into the same tube with 0.6 CV of 300 mM imidazole desalting buffer. The resulting purified protein was concentrated to 100 μL using a 10K molecular weight cutoff (MWCO) 0.5 mL Pierce Protein concentrator (ThermoFisher), desalted into PBS using 7K MWCO 0.5 mL Zeba Spin Desalting column (ThermoFisher), and stored at 4 °C until use.

For purification of hinge-Fc^{DQNAT} from IVG and CFGpS reactions, 1 μL of well-mixed MabSelect Resin (Cytiva) was equilibrated with equilibration buffer (0.1 M NaH_2PO_4, 0.15 M NaCl, pH 8, sterile filtered) per 2 μL of IVG or CFGpS reaction product. The resin slurry was added to a 10-mL Poly prep Chromatography Column (Bio-Rad). The column was then capped, filled with equilibration buffer, and incubated for 5 min to let the resin settle. After incubation, the column was washed with 10 mL of equilibration buffer. The reaction product and the equilibration buffer were mixed 1:1 (v/v) and flowed through the column. The column was then washed with 20 column volumes (CV) of equilibration buffer. Meanwhile, tubes for collecting elution fractions were prepared with 0.08 CV neutralizing buffer. The product was eluted in 3 fractions by incubating 0.8 CV elution buffer for 1 min with the resin and subsequently flowing it through the column. The fractions found to contain significant quantities of protein based on the absorbance at 280 nm were combined and concentrated to ~130 μL using a 10K MWCO 0.5 mL Pierce Protein concentrator (ThermoFisher), buffer exchanged into PBS using a 0.5 mL 7K MWCO Zeba Spin Desalting column (ThermoFisher) and stored at 4 °C until further use.

Immunoblotting. All immunoblots were performed using protein samples that were purified as described above. RNase A samples were solubilized in 10% (v/v) β-mercaptoethanol (BME) in 4× lithium dodecyl sulfate (LDS) buffer and subsequently heated at 98 °C for 10 min. Hinge-Fc samples were solubilized in 50 mM IAM in 4× LDS buffer and subsequently heated at 75 °C for 5 min. All samples were run on Bolt Bis-Tris Plus gels (ThermoFisher) and transferred to 0.2 μm Immobilon-P PVDF transfer membranes (Millipore Sigma) via a semi-dry transfer apparatus (Bio-Rad). All membranes were then blocked overnight in 5% non-fat dairy milk in TBST (Tris-buffer saline (TBS) solution (10 mM Tris-base, 150 mM NaCl, pH 7.5) plus 0.05% (v/v) Tween-20) at 4 °C. The following antibodies were used for immunoblotting and prepared in TBST unless otherwise specified: polyhistidine (6×-His) tag-specific polyclonal antibody conjugated to horseradish peroxidase (HRP) (1:10,000 dilution; Abcam, cat # ab1187); F(ab')2-goat antihuman IgG (H + L) secondary antibody conjugated to HRP (1:5000 dilution; ThermoFisher, cat # A24464) prepared in 5% nonfat dairy milk in TBST, *C. jejuni* heptasaccharide glycan-specific antiserum hR6 (1:10,000 dilution; kind gift of Marcus Aebi, ETH-Zürich),[34] and goat anti-rabbit IgG conjugated to HRP (1:7500 dilution; Abcam, cat # ab7083). For anti-His and anti-IgG blots, the membrane was washed 3 times with TBST and then the primary antibody was incubated for at least 3 h with shaking at room temperature (RT). For antiglycan blots, the hR6 serum was incubated with the membrane for 1 h with shaking at RT. The membrane was then washed 3 times in TBST for 10 min with shaking at RT, and then incubated for 1 h in the anti-rabbit IgG antibody solution with shaking at RT. The final wash prior to imaging was 6 times in TBST for 5 min with shaking at RT for all membranes. Images were obtained by chemiluminescence detection on a Chemidoc XRS+ or MP imaging system (Bio-Rad) using two-part Western ECL substrate (Bio-Rad).

Mass Spectrometry. Intact glycoprotein mass spectrometry was performed similarly to past protocols.[41,67] The glycosylation status of $GalNAc_5GlcNAc$-hinge-Fc was analyzed via LC-ESI-MS by treatment with DTT to reduce the protein and IdeS to cleave the protein at a specific site between the hinge and Fc. Briefly, DTT treatment was performed with 10 mM DTT for 10 min at 37 °C, while IdeS treatment was performed by adding IdeS at a ratio of sample/IdeS of 1:10 (w/w) and incubating for 10 min at 37 °C. Next, GalNAc removal was performed using exo-α-*N*-acetylgalactosaminidase (New England Biolabs) whereby $GalNAc_5GlcNAc$-hinge-Fc (100 μg) was mixed with BSA, GlycoBuffer 1, and exo-α-*N*-acetylgalactosaminidase (100 U) according to manufacturer's instructions. The reaction mixture was incubated at 37 °C and the reaction was monitored by LC-ESI-MS over the course of 1 h.

For glycoproteomic tandem mass spectrometry, partially purified proteins in 1× PBS solution were reduced by heating in 25 mM DTT at 50 °C for 45 min, then cooled down to room temperature and immediately alkylated by incubating with 90 mM iodoacetamide (IAA) at room temperature in the dark for 20 min. Samples were loaded on the top of 3-kDa MWCO filters and desalted by passing through with 800 μL of 50 mM ammonium bicarbonate (Ambic). Proteins were recovered from the filters and reconstituted as 1 μg/μL solution in 50 mM Ambic. Sequencing grade trypsin was added to samples at a 1:20 ratio and digestion was performed at 37 °C overnight. Trypsin activity was terminated by heating at 100 °C for 5 min. Cooled samples were reconstituted in LC−MS grade 0.1% formic acid (FA) as a 0.1 μg/μL solution and passed through 0.2 μm filters. LC−MS/MS was carried out on an Ultimate 3000 RSLCnano low-flow liquid chromatography system coupled with Orbitrap Tribrid Eclipse mass spectrometer via a Nanospray Flex ion source. Samples were trap-loaded on a 2 μm pore size 75 μm × 150 mm Acclaim PepMap 100 C18 nanoLC column. The column was equilibrated at 0.300 μL/min flowrate with 96% Buffer A (0.1% FA) and 4% Buffer B (80% acetonitrile (ACN) with 0.1% FA). A 60-min gradient in which Buffer B ramped from 4% to 62.5% was used for peptide separation. To scrutinize the expected glycan attachment at the expected sequon, a higher collision energy dissociation (HCD) product-triggered collision induced dissociation (CID) (HCDpdCID) MS/MS fragmentation cycle in a 3-s frame was used. Precursors were scanned in Orbitrap at 120,000 resolution and fragments were detected in Orbitrap at 30,000 resolution.[68]

https://doi.org/10.1021/acssynbio.5c00229
ACS Synth. Biol. 2025, 14, 2354−2367

LC−MS/MS data was searched in Byonic (v5.5.2) and manually inspected in Freestyle (v1.8 SP1). Human hinge-Fc^{DQNAT}, *E. coli* chaperone GroEL, and common contaminant sequences with fully reversed decoy were used for peptide backbone identification. The precursor mass tolerance was set at 5 ppm, while the fragment mass tolerance was allowed as 20 ppm. Glycan compositions HexNAc(1−10) were considered as the potential *N*-glycan list. Protein list output was set with a cutoff at 1% false detection rate (FDR) or 20 reverse sequences, whichever came last. Only fully specific tryptic peptides with up to two mis-cleavages were considered. Carbamidomethylation on cysteine was considered as a fixed modification. Oxidation on methionine, deamidation on asparagine and glutamine were considered as variable modifications. Peptide identity and modifications were annotated by Byonic, followed by manual inspection of peptide backbone *b*/*y* ions (including labile fragments losing of full or partial glycan moiety), glycan oxonium ions, and glycopeptide *y*-ion neutral losses.[69] Relative abundance of glycoforms reported were based on area under the curve of 2−4 charged extracted ion chromatogram (XIC) peaks processed in Freestyle using the protein Averagine model. Based on high confidence aglycosylated and glycosylated DQNAT peptide retention time, all possible precursors of pep + HexNAc(1−15) were explored and evaluated.[70]

■ ASSOCIATED CONTENT

Supporting Information

The Supporting Information is available free of charge at https://pubs.acs.org/doi/10.1021/acssynbio.5c00229.

Cell-free expression of catalytically inactivated RNase A variant analyzed via Western blot, effect of flippase expression on RNase A glycosylation, structural models of aglycosylated and glycosylated hinge-Fc^{DQNAT}, SDS-PAGE and Western blot analysis of purified hinge-Fc^{DQNAT}, LCMS analysis of glycosylated hinge-Fc^{DQNAT}, and DNA sequences of plasmids used in the study (PDF)

■ AUTHOR INFORMATION

Corresponding Author

Matthew P. DeLisa − *Robert Frederick Smith School of Chemical and Biomolecular Engineering, Cornell University, Ithaca, New York 14853, United States; Cornell Institute of Biotechnology, Cornell University, Ithaca, New York 14853, United States;* orcid.org/0000-0003-3226-1566; Phone: 607-254-8560; Email: md255@cornell.edu

Authors

Erik J. Bidstrup − *Robert Frederick Smith School of Chemical and Biomolecular Engineering, Cornell University, Ithaca, New York 14853, United States;* orcid.org/0000-0001-9014-2042

Kyle Hill − *Cell-Free Protein Synthesis and Microbial Process Development, National Resilience Inc., Oakland, California 94606, United States*

Chandra K. Bandi − *Robert Frederick Smith School of Chemical and Biomolecular Engineering, Cornell University, Ithaca, New York 14853, United States*

D. Natasha Owitipana − *Department of Chemistry and Biochemistry, University of Maryland, College Park, Maryland 1220742, United States;* orcid.org/0000-0002-3701-3222

Alina Chisti − *Robert Frederick Smith School of Chemical and Biomolecular Engineering, Cornell University, Ithaca, New York 14853, United States*

Rochelle Aw − *Department of Bioengineering, Stanford University, Stanford, California 94305, United States*

Xu Yang − *Complex Carbohydrate Research Center, University of Georgia, Athens, Georgia 30602-4712, United States;* orcid.org/0000-0001-9802-9845

Parastoo Azadi − *Complex Carbohydrate Research Center, University of Georgia, Athens, Georgia 30602-4712, United States;* orcid.org/0000-0002-6166-9432

Michael C. Jewett − *Department of Bioengineering, Stanford University, Stanford, California 94305, United States;* orcid.org/0000-0003-2948-6211

Lai-Xi Wang − *Department of Chemistry and Biochemistry, University of Maryland, College Park, Maryland 1220742, United States;* orcid.org/0000-0003-4293-5819

Weston Kightlinger − *Cell-Free Protein Synthesis and Microbial Process Development, National Resilience Inc., Oakland, California 94606, United States*

Complete contact information is available at: https://pubs.acs.org/10.1021/acssynbio.5c00229

Author Contributions

E.J.B. designed research, performed research, analyzed data, and wrote the paper. K.H., D.N.O., A.C., R.A., and X.Y. designed research, performed research, and analyzed data. P.A., M.C.J., L.-X.W., and W.K. designed and directed research and analyzed data. M.P.D. designed and directed research, analyzed data, and wrote the paper. All authors read and approved the final manuscript.

Notes

The authors declare the following competing financial interest(s): M.P.D. and M.C.J. have financial interests in Gauntlet, Inc. and Resilience, Inc. M.P.D. also has financial interests in Disply Bio, LLC, Glycobia, Inc., UbiquiTx, Inc., and Versatope Therapeutics, Inc. M.P.D.s and M.C.J.s interests are reviewed and managed by Cornell University and Stanford University, respectively, in accordance with their conflict-of-interest policies. All other authors declare no competing interests.

■ ACKNOWLEDGMENTS

We thank Markus Aebi (ETH Zürich) for providing antiserum used in this work as well as Sophia Hulbert and Yong Hyun Kwon (Cornell University) for construction of a strain and plasmid used in this work. This work was supported by the Defense Advanced Research Projects Agency (DARPA contract W911NF-23-2-0039 to M.C.J. and M.P.D.), the Defense Threat Reduction Agency (grant HDTRA1-20-10004 to M.C.J. and M.P.D.), the National Science Foundation (grant CBET-1605242 to M.P.D., grant CBET-1936823 to M.C.J. and M.P.D., and grant DMR-1933525 to P.A.), and the National Institutes of Health (grant R24GM137782 to P.A.). E.J.B. was supported by an NIH/NIGMS Chemical Biology Interface Training Grant (T32GM138826) and an NSF Graduate Research Fellowship (DGE-2139899).

REFERENCES

(1) Perez-Pinera, P.; Han, N.; Cleto, S.; Cao, J.; Purcell, O.; Shah, K. A.; Lee, K.; Ram, R.; Lu, T. K. Synthetic biology and microbioreactor platforms for programmable production of biologics at the point-of-care. *Nat. Commun.* **2016**, *7*, 12211.

(2) Crowell, L. E.; Lu, A. E.; Love, K. R.; Stockdale, A.; Timmick, S. M.; Wu, D.; Wang, Y. A.; Doherty, W.; Bonnyman, A.; Vecchiarello, N.; et al. On-demand manufacturing of clinical-quality biopharmaceuticals. *Nat. Biotechnol.* **2018**, *36*, 988−995.

(3) Pardee, K.; Slomovic, S.; Nguyen, P. Q.; Lee, J. W.; Donghia, N.; Burrill, D.; Ferrante, T.; McSorley, F. R.; Furuta, Y.; Vernet, A.; et al. Portable, on-demand biomolecular manufacturing. *Cell* **2016**, *167*, 248−259.e12.

(4) Salehi, A. S.; et al. Cell-free protein synthesis of a cytotoxic cancer therapeutic: Onconase production and a just-add-water cell-free system. *Biotechnol. J.* **2016**, *11*, 274−281.

(5) Adiga, R.; et al. Point-of-care production of therapeutic proteins of good-manufacturing-practice quality. *Nat. Biomed. Eng.* **2018**, *2*, 675−686.

(6) Walsh, G.; Walsh, E. Biopharmaceutical benchmarks 2022. *Nat. Biotechnol.* **2022**, *40*, 1722−1760.

(7) Varki, A. Biological roles of glycans. *Glycobiology* **2017**, *27*, 3−49.

(8) Sola, R. J.; Griebenow, K. Effects of glycosylation on the stability of protein pharmaceuticals. *J. Pharm. Sci.* **2009**, *98*, 1223−1245.

(9) Jefferis, R. Glycosylation as a strategy to improve antibody-based therapeutics. *Nat. Rev. Drug Discovery* **2009**, *8*, 226−234.

(10) Sinclair, A. M.; Elliott, S. Glycoengineering: the effect of glycosylation on the properties of therapeutic proteins. *J. Pharm. Sci.* **2005**, *94*, 1626−1635.

(11) Jaroentomeechai, T.; Stark, J. C.; Natarajan, A.; Glasscock, C. J.; Yates, L. E.; Hsu, K. J.; Mrksich, M.; Jewett, M. C.; DeLisa, M. P. Single-pot glycoprotein biosynthesis using a cell-free transcription-translation system enriched with glycosylation machinery. *Nat. Commun.* **2018**, *9*, 2686.

(12) Hershewe, J. M.; Warfel, K. F.; Iyer, S. M.; Peruzzi, J. A.; Sullivan, C. J.; Roth, E. W.; DeLisa, M. P.; Kamat, N. P.; Jewett, M. C. Improving cell-free glycoprotein synthesis by characterizing and enriching native membrane vesicles. *Nat. Commun.* **2021**, *12*, 2363.

(13) Kightlinger, W.; Duncker, K. E.; Ramesh, A.; Thames, A. H.; Natarajan, A.; Stark, J. C.; Yang, A.; Lin, L.; Mrksich, M.; DeLisa, M. P.; et al. A cell-free biosynthesis platform for modular construction of protein glycosylation pathways. *Nat. Commun.* **2019**, *10*, 5404.

(14) Natarajan, A.; et al. Engineering orthogonal human O-linked glycoprotein biosynthesis in bacteria. *Nat. Chem. Biol.* **2020**, *16*, 1062−1070.

(15) Stark, J. C.; et al. Rapid biosynthesis of glycoprotein therapeutics and vaccines from freeze-dried bacterial cell lysates. *Nat. Protoc.* **2023**, *18*, 2374−2398.

(16) Stark, J. C.; Jaroentomeechai, T.; Moeller, T. D.; Hershewe, J. M.; Warfel, K. F.; Moricz, B. S.; Martini, A. M.; Dubner, R. S.; Hsu, K. J.; Stevenson, T. C.; et al. On-demand biomanufacturing of protective conjugate vaccines. *Sci. Adv.* **2021**, *7*, No. eabe9444.

(17) Williams, A. J.; Warfel, K. F.; Desai, P.; Li, J.; Lee, J. J.; Wong, D. A.; Nguyen, P. M.; Qin, Y.; Sobol, S. E.; Jewett, M. C.; et al. A low-cost recombinant glycoconjugate vaccine confers immunogenicity and protection against enterotoxigenic Escherichia coli infections in mice. *Front. Mol. Biosci.* **2023**, *10*, 1085887.

(18) Warfel, K. F.; et al. A low-cost, thermostable, cell-free protein synthesis platform for on-demand production of conjugate vaccines. *ACS Synth. Biol.* **2023**, *12*, 95−107.

(19) Kowarik, M.; et al. N-linked glycosylation of folded proteins by the bacterial oligosaccharyltransferase. *Science* **2006**, *314*, 1148−1150.

(20) Silverman, J. M.; Imperiali, B. Bacterial N-glycosylation efficiency Is dependent on the structural context of target sequons. *J. Biol. Chem.* **2016**, *291*, 22001−22010.

(21) Li, M.; Zheng, X.; Shanker, S.; Jaroentomeechai, T.; Moeller, T. D.; Hulbert, S. W.; Koçer, I.; Byrne, J.; Cox, E. C.; Fu, Q.; et al. Shotgun scanning glycomutagenesis: A simple and efficient strategy for constructing and characterizing neoglycoproteins. *Proc. Natl. Acad. Sci. U.S.A.* **2021**, *118*, No. e2107440118.

(22) Valderrama-Rincon, J. D.; et al. An engineered eukaryotic protein glycosylation pathway in Escherichia coli. *Nat. Chem. Biol.* **2012**, *8*, 434−436.

(23) Pratama, F.; Linton, D.; Dixon, N. Genetic and process engineering strategies for enhanced recombinant N-glycoprotein production in bacteria. *Microb. Cell Fact.* **2021**, *20*, 198.

(24) Shrimal, S.; Cherepanova, N. A.; Gilmore, R. Cotranslational and posttranslocational N-glycosylation of proteins in the endoplasmic reticulum. *Semin. Cell Dev. Biol.* **2015**, *41*, 71−78.

(25) Cherepanova, N. A.; Venev, S. V.; Leszyk, J. D.; Shaffer, S. A.; Gilmore, R. Quantitative glycoproteomics reveals new classes of STT3A- and STT3B-dependent N-glycosylation sites. *J. Cell Biol.* **2019**, *218*, 2782−2796.

(26) Williams, R. L.; Greene, S. M.; McPherson, A. The crystal structure of ribonuclease B at 2.5-A resolution. *J. Biol. Chem.* **1987**, *262*, 16020−16031.

(27) Ollis, A. A.; Zhang, S.; Fisher, A. C.; DeLisa, M. P. Engineered oligosaccharyltransferases with greatly relaxed acceptor-site specificity. *Nat. Chem. Biol.* **2014**, *10*, 816−822.

(28) Thompson, J. E.; Raines, R. T. Value of general Acid-base catalysis to ribonuclease a. *J. Am. Chem. Soc.* **1994**, *116*, 5467−5468.

(29) Zhang, G.; Brokx, S.; Weiner, J. H. Extracellular accumulation of recombinant proteins fused to the carrier protein YebF in Escherichia coli. *Nat. Biotechnol.* **2006**, *24*, 100−104.

(30) Klink, T. A.; Woycechowsky, K. J.; Taylor, K. M.; Raines, R. T. Contribution of disulfide bonds to the conformational stability and catalytic activity of ribonuclease A. *Eur. J. Biochem.* **2000**, *267*, 566−572.

(31) Lobstein, J.; Emrich, C. A.; Jeans, C.; Faulkner, M.; Riggs, P.; Berkmen, M. SHuffle, a novel Escherichia coli protein expression strain capable of correctly folding disulfide bonded proteins in its cytoplasm. *Microb. Cell Fact.* **2012**, *11*, 753.

(32) Robinson, M. P.; et al. Efficient expression of full-length antibodies in the cytoplasm of engineered bacteria. *Nat. Commun.* **2015**, *6*, 8072.

(33) Dopp, J. L.; Reuel, N. F. Simple, functional, inexpensive cell extract for in vitro prototyping of proteins with disulfide bonds. *Biochem. Eng. J.* **2020**, *164*, 107790.

(34) Schwarz, F.; et al. Relaxed acceptor site specificity of bacterial oligosaccharyltransferase in vivo. *Glycobiology* **2011**, *21*, 45−54.

(35) Rothblatt, J. A.; Meyer, D. I. Secretion in yeast: reconstitution of the translocation and glycosylation of alpha-factor and invertase in a homologous cell-free system. *Cell* **1986**, *44*, 619−628.

(36) Bergman, L. W.; Kuehl, W. M. Co-translational modification of nascent immunoglobulin heavy and light chains. *J. Supramol. Struct.* **1979**, *11*, 9−24.

(37) Borrok, M. J.; Jung, S. T.; Kang, T. H.; Monzingo, A. F.; Georgiou, G. Revisiting the role of glycosylation in the structure of human IgG Fc. *ACS Chem. Biol.* **2012**, *7*, 1596−1602.

(38) Feige, M. J.; et al. Structure of the murine unglycosylated IgG1 Fc fragment. *J. Mol. Biol.* **2009**, *391*, 599−608.

(39) Vidarsson, G.; Dekkers, G.; Rispens, T. IgG subclasses and allotypes: from structure to effector functions. *Front. Immunol.* **2014**, *5*, 520.

(40) Fisher, A. C.; et al. Production of secretory and extracellular N-linked glycoproteins in Escherichia coli. *Appl. Environ. Microbiol.* **2011**, *77*, 871−881.

(41) Sotomayor, B.; et al. Discovery of a single-subunit oligosaccharyltransferase that enables glycosylation of full-length IgG antibodies in Escherichia coli. *bioRxiv* **2024**.

(42) Ollis, A. A.; Chai, Y.; Natarajan, A.; Perregaux, E.; Jaroentomeechai, T.; Guarino, C.; Smith, J.; Zhang, S.; DeLisa, M. P. Substitute sweeteners: diverse bacterial oligosaccharyltransferases with unique N-glycosylation site preferences. *Sci. Rep.* **2015**, *5*, 15237.

(43) Schwarz, F.; et al. A combined method for producing homogeneous glycoproteins with eukaryotic N-glycosylation. *Nat. Chem. Biol.* **2010**, *6*, 264−266.

https://doi.org/10.1021/acssynbio.5c00229
ACS Synth. Biol. 2025, 14, 2354−2367

(44) Sotomayor, B.; et al. Glycosylation of full-length IgG antibodies in bacteria enabled by a single-subunit oligosaccharyltransferase from Desulfovibrio marinus. *Nat. Commun.* **2025** (accepted for publication).
(45) Dudley, Q. M.; Anderson, K. C.; Jewett, M. C. Cell-free mixing of Escherichia coli crude extracts to prototype and rationally engineer high-titer mevalonate synthesis. *ACS Synth. Biol.* **2016**, *5*, 1578−1588.
(46) Bergonzo, C.; Hoopes, J. T.; Kelman, Z.; Gallagher, D. T. Effects of glycans and hinge on dynamics in the IgG1 Fc. *J. Biomol. Struct. Dyn.* **2024**, *42*, 12571−12579.
(47) Groff, D.; et al. Engineering toward a bacterial "endoplasmic reticulum" for the rapid expression of immunoglobulin proteins. *MAbs* **2014**, *6*, 671−678.
(48) Ruiz-Canada, C.; Kelleher, D. J.; Gilmore, R. Cotranslational and posttranslational N-glycosylation of polypeptides by distinct mammalian OST isoforms. *Cell* **2009**, *136*, 272−283.
(49) Braunger, K.; et al. Structural basis for coupling protein transport and N-glycosylation at the mammalian endoplasmic reticulum. *Science* **2018**, *360*, 215−219.
(50) Shrimal, S.; Cherepanova, N. A.; Mandon, E. C.; Venev, S. V.; Gilmore, R. Asparagine-linked glycosylation is not directly coupled to protein translocation across the endoplasmic reticulum in Saccharomyces cerevisiae. *Mol. Biol. Cell* **2019**, *30*, 2626−2638.
(51) Liu, C. P.; et al. Glycoengineering of antibody (Herceptin) through yeast expression and in vitro enzymatic glycosylation. *Proc. Natl. Acad. Sci. U. S. A.* **2018**, *115*, 720−725.
(52) delCardayre, S. B.; et al. Engineering ribonuclease A: production, purification and characterization of wild-type enzyme and mutants at Gln11. *Protein Eng.* **1995**, *8*, 261−273.
(53) Underwood, K. A.; Swartz, J. R.; Puglisi, J. D. Quantitative polysome analysis identifies limitations in bacterial cell-free protein synthesis. *Biotechnol. Bioeng.* **2005**, *91*, 425−435.
(54) Chung, S. S.; et al. Ribosome stalling of N-linked glycoproteins in cell-free extracts. *ACS Synth. Biol.* **2022**, *11*, 3892−3899.
(55) Craig, E. A.; Eisenman, H. C.; Hundley, H. A. Ribosome-tethered molecular chaperones: the first line of defense against protein misfolding? *Curr. Opin. Microbiol.* **2003**, *6*, 157−162.
(56) Altendorf, K. H.; Staehelin, L. A. Orientation of membrane vesicles from Escherichia coli as detected by freeze-cleave electron microscopy. *J. Bacteriol.* **1974**, *117*, 888−899.
(57) Jewett, M. C.; Calhoun, K. A.; Voloshin, A.; Wuu, J. J.; Swartz, J. R. An integrated cell-free metabolic platform for protein production and synthetic biology. *Mol. Syst. Biol.* **2008**, *4*, 220.
(58) Jewett, M. C.; Swartz, J. R. Mimicking the Escherichia coli cytoplasmic environment activates long-lived and efficient cell-free protein synthesis. *Biotechnol. Bioeng.* **2004**, *86*, 19−26.
(59) Muller, M.; Blobel, G. In vitro translocation of bacterial proteins across the plasma membrane of Escherichia coli. *Proc. Natl. Acad. Sci. U. S. A.* **1984**, *81*, 7421−7425.
(60) Anthony, R. M.; et al. Recapitulation of IVIG anti-inflammatory activity with a recombinant IgG Fc. *Science* **2008**, *320*, 373−376.
(61) Feldman, M. F.; et al. Engineering N-linked protein glycosylation with diverse O antigen lipopolysaccharide structures in Escherichia coli. *Proc. Natl. Acad. Sci. U. S. A.* **2005**, *102*, 3016−3021.
(62) Schoborg, J. A.; et al. A cell-free platform for rapid synthesis and testing of active oligosaccharyltransferases. *Biotechnol. Bioeng.* **2018**, *115*, 739−750.
(63) Bidstrup, E. J.; et al. Cell-free systems for the production of glycoproteins. *Methods Mol. Biol.* **2024**, *2762*, 309−328.
(64) Martin, R. W.; et al. Development of a CHO-based cell-free platform for synthesis of active monoclonal antibodies. *ACS Synth. Biol.* **2017**, *6*, 1370−1379.
(65) Kwon, Y. C.; Jewett, M. C. High-throughput preparation methods of crude extract for robust cell-free protein synthesis. *Sci. Rep.* **2015**, *5*, 8663.
(66) Zawada, J. F.; et al. Microscale to manufacturing scale-up of cell-free cytokine production–a new approach for shortening protein production development timelines. *Biotechnol. Bioeng.* **2011**, *108*, 1570−1578.
(67) Giddens, J. P.; Lomino, J. V.; DiLillo, D. J.; Ravetch, J. V.; Wang, L. X. Site-selective chemoenzymatic glycoengineering of Fab and Fc glycans of a therapeutic antibody. *Proc. Natl. Acad. Sci. U. S. A.* **2018**, *115*, 12023−12027.
(68) Klein, J.; Zaia, J. Relative retention time estimation improves N-glycopeptide identifications by LC-MS/MS. *J. Proteome Res.* **2020**, *19*, 2113−2121.
(69) Quaranta, A.; et al. N-glycosylation profiling of intact target proteins by high-resolution mass spectrometry (MS) and glycan analysis using ion mobility-MS/MS. *Analyst* **2020**, *145*, 1737−1748.
(70) Lee, L. Y.; et al. Toward automated N-glycopeptide identification in glycoproteomics. *J. Proteome Res.* **2016**, *15*, 3904−3915.

https://doi.org/10.1021/acssynbio.5c00229
ACS Synth. Biol. 2025, 14, 2354−2367